RSC Advances

PAPER

View Article Online
View Journal | View Issue

Cite this: *RSC Adv.*, 2022, **12**, 10625

Preparation of epoxy/ZrO_2 composite coating on the Q235 surface by electrostatic spraying and its corrosion resistance in 3.5% NaCl solution

Jipeng Wu, Guojun Ji * and Qiang Wu

Received 23rd February 2022
Accepted 24th March 2022

DOI: 10.1039/d2ra01220k

rsc.li/rsc-advances

The epoxy coating containing ZrO_2 nanoparticles modified with 3-aminopropyltriethoxysilane (APTES) was prepared by electrostatic spraying on the surface of Q235 mild steel. The effect of the concentration of APTES-modified ZrO_2 nanoparticles on the corrosion resistance of epoxy coating was characterized and tested by FTIR spectroscopy, scanning electron microscopy (SEM) and electrochemical impedance spectroscopy (EIS). The results show that nano ZrO_2 was successfully modified by a silane coupling agent. By adding an appropriate amount of APTES to modify nano ZrO_2 in epoxy coating could significantly improve the corrosion resistance of the Q235 surface. When the mass fraction of nano ZrO_2 is 2%, the composite coating shows the highest impedance value of about 1.0×10^5 Ω cm^2 to achieve the best corrosion resistance.

1. Introduction

Low carbon steel is widely used in daily life. Due to its low cost and good physical and mechanical properties, it is also widely used in automobile, construction, petroleum, ship, sea bridge, shipping and chemical industries.[1,2] Corrosion is the main problem of low carbon steel failure. Due to the corrosion failure of low carbon steel, a lot of materials and funds are wasted. Epoxy resin is widely used for the surface protection of low carbon steel due to its acid and alkali resistance and good adhesion to the substrate.[3–6] Epoxy resin can form an effective protective film between low carbon steel and corrosive ions to protect low carbon steel from the corrosion of corrosive ions. However, with the expansion of the application scope of epoxy resin and the complexity of the application environment, more requirements are put forward for its anti-corrosion performance. In practical application, due to the pinhole and porosity in its structure, the pure epoxy resin coating is easy to degrade after long-time immersion and can penetrate small corrosive medium molecules, such as water, oxygen and ions, which may cause metal corrosion under the coating.[7]

In recent years, nanoparticles have shown excellent properties in the coating system, including excellent barrier, flame retardant and wear resistance properties.[8] Therefore, the modification of epoxy resin by nano inorganic fillers (including nano TiO_2,[9] nano SiO_2,[10] and graphene[11–13]) to improve the corrosion resistance of the coating has become a hot topic in the application of organic coatings. However, the surface energy of nanoparticles is high and easy to agglomerate, which may weaken the role of nanoparticles. Therefore, the dispersion of nanoparticles in epoxy resin coating is the key factor to prepare epoxy coating with excellent performance. At present, the modification of nanoparticles with a silane coupling agent is one of the mainstream methods to improve the dispersion of nanoparticles.[14,15]

Among all nanoparticles, ZrO_2 nanoparticles are one of the most promising for anti-corrosion coating.[16–19] It has great specific surface area, high corrosion resistance, excellent mechanical properties and biocompatibility. Dispersing nanoparticles into epoxy resin not only enhances the mechanical properties of epoxy resin but also effectively improves its corrosion resistance.[20–22] In this study, ZrO_2 nanoparticles were modified by 3-aminopropyl triethoxysilane to ensure the uniform dispersion of ZrO_2 nanoparticles in the epoxy coating. The epoxy resin coating containing modified ZrO_2 nanoparticles on the surface of a Q235 steel plate was prepared by electrostatic spraying, Fourier infrared spectroscopy, and scanning electron microscopy. The coating was characterized by electrochemical tests and other characterization methods. The effect of the concentration of modified ZrO_2 nanoparticles on the corrosion resistance of epoxy resin coating was studied, and the corrosion resistance mechanism of the coating was explored.

2. Experimental

2.1 Preparation of modified ZrO_2 nanoparticles

5 g of ZrO_2 nanoparticles was added to 150 mL of absolute ethanol. After ultrasonically dispersing the mixture for 30 min, 3 g APTES was added and ultrasonic dispersion continued for 1 h. After magnetic stirring at 60 °C for 8 h, the obtained

College of Chemical Engineering, Inner Mongolia University of Technology, Hohhot, 010051, China. E-mail: jgj@imut.edu.cn

nanoparticles were centrifuged, the centrifuged precipitate was washed with absolute ethanol for 2–3 times to remove excess APTES, and was finally dried in an oven at 70 °C to obtain modified ZrO_2 nanoparticles.

2.2 Preparation of composite coating

The matrix used in this experiment is a Q235 steel plate (99.523% Fe, 0.16% C, 0.08% Si, 0.21% Mn, 0.015% P, 0.012% s), and the size is 20 mm × 20 mm × 1 mm. Prior to the experiment, the Q235 steel plate with 400 mesh and 1200 mesh sandpapers was polished, respectively. Then, it was put into absolute ethanol for 20 min of ultrasonic cleaning, followed by putting it in the oven and blow drying for standby. As shown in Fig. 1, a certain amount of modified ZrO_2 was dispersed into 150 mL absolute ethanol under an ultrasonic dispersion treatment for 30 min. Then, E20 epoxy resin was added in a constant water bath at 80 °C and stirred magnetically for 12 h. The mixture was dried, crushed and screened, and an appropriate amount of dicyandiamine curing agent was added in an epoxy : dicyanodiamine ratio of 20 : 3. An electrostatic powder layer was formed on the Q235 steel plate by electrostatic spraying under 30 kV electrostatic voltage and 0.6 MPa air pressure. The distance between the spray gun and the steel plate during spraying is 30 cm. After curing at 160 °C for 2 h, a uniform coating was formed. The uncoated Q235 steel plate and epoxy resin coating were used as the reference samples for the experiment.

2.3 Characterization of powder and coating

The FT-IR spectra of ZrO_2 nanoparticles were recorded at 4000 to 500 cm^{-1} using a Fourier transform infrared spectrometer (nexue 870, negoly, USA). The thickness and surface morphology of the coating samples were recorded by an s3400 scanning electron microscope (SEM, Japan Juchang Manufacturing Institute, working voltage 20 kV).

2.4 Test of corrosion resistance of coating

The electrochemical corrosion test method was adopted. This test aims to simulate the harsh atmospheric conditions when the coating is exposed to the marine environment. Considering that the content of sodium chloride in normal seawater is about 3.5%, the corrosive medium in this electrochemical test is 3.5% NaCl solution. The corrosion protection effect of the samples in 3.5% NaCl solution was evaluated by the electrochemical corrosion test method and CS Series electrochemical workstation (Wuhan Coster instrument). The standard three electrode system was adopted for the test: the coated sample was used as the working electrode (we), a platinum sheet (PT) was used as the auxiliary electrode (CE), and an Ag/AgCl electrode was used as the reference electrode (RE). The test temperature of the electrochemical experiment is 25 °C, the scanning rate of potentiodynamic polarization is 2 mV s^{-1}, and the applied potential is −1.5 V to +0.0 V. The exposed area of the sample is 1.0 cm^2 and the frequency range of electrochemical impedance spectrum is 10^{-2} to 10^5 Hz.

3. Results and discussion

3.1 FTIR spectroscopy

Fig. 2 shows the infrared spectra of ZrO_2 and APTES-modified ZrO_2. The results show that the strong vibration peak at 3404 cm^{-1} can be attributed to the tensile vibration of –OH on the ZrO_2 surface; the absorption peak at 2933 cm^{-1} can be attributed to the tensile vibration of C–H in APTES. The peaks at 1114 cm^{-1}, 1042 cm^{-1}, and 749 cm^{-1}indicate the presence of

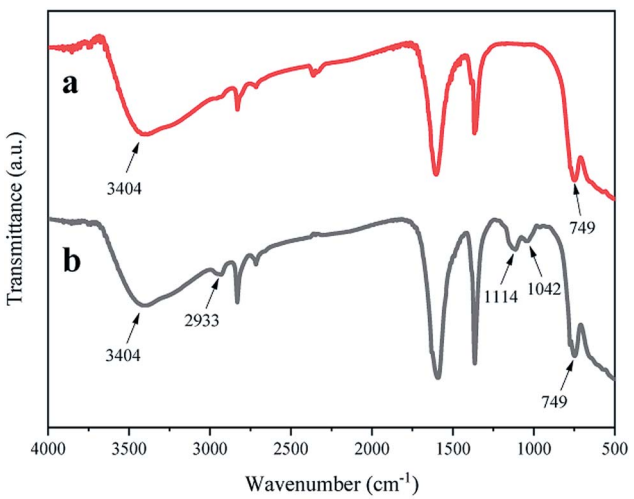

Fig. 2 FTIR spectra of untreated (a) and APTES-modified (b) ZrO_2 nanoparticles.

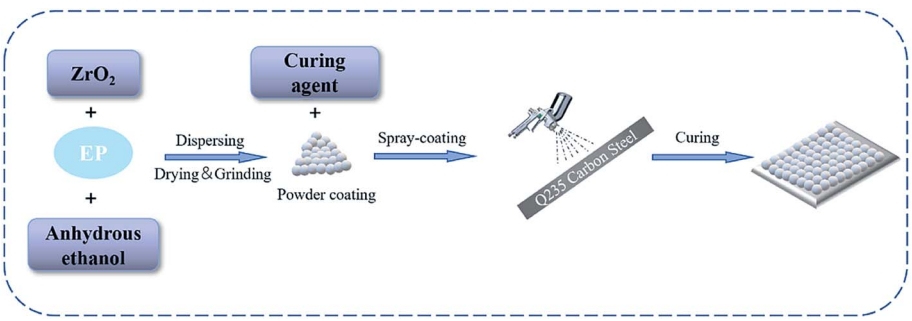

Fig. 1 Preparation diagram of composite coating.

Si–O–Si, Zr–O–Si,[23] and the Zr–O–Zr tensile vibrations,[24], respectively. In conclusion, APTES was successfully anchored on the surface of nano ZrO_2 through chemical bonds.

3.2 Dispersion stability test in an organic solvent

In order to better reflect the dispersion of ZrO_2 modified by APTES, the samples of unmodified and modified ZrO_2 nanoparticles were subjected to standing test after ultrasonic dispersion for 1 h. The test results are shown in Fig. 3.

The unmodified ZrO_2 nanoparticles dispersed in absolute ethanol began to appear delaminated after standing for 3 min, and obvious precipitation could be observed after 10 min. ZrO_2 dispersed in the solution basically precipitated in about 4 h. Another group of ZrO_2 nanoparticles dispersed in absolute ethanol and modified by APTES were still well dispersed suspensions after standing and settling for 48 h, without obvious stratification. This phenomenon shows that the stability of nanoparticles in organic solvents can be increased after the nanoparticles are modified by a silane coupling agent. This proves that the silane coupling agent APTES has modified ZrO_2.[25]

3.3 SEM

The cross section of the composite coating sample formed by electrostatic spraying was obtained after treatment and observed by a scanning electron microscope. The cross section morphology is shown in Fig. 3. Based on the image observation and measurement, the coating thickness is about 110 μm.

In order to observe the microstructure of the coating, the coating surfaces of different samples were characterized by SEM, as shown in Fig. 4.

Fig. 5(a)–(e) are the SEM photos of epoxy resin coating after adding different contents of APTES-modified ZrO_2. Moreover, in Fig. 5(a)–(e), it is found that there are pores present on the coating surface. These pores are formed on the surface of the coating due to the accumulation of powder coatings and the inclusion of a small amount of air in the coating gap during electrostatic spraying. Therefore, during the curing process of the coating, a small amount of air dissolved in the coating escapes forming tiny bubbles that eventually break.

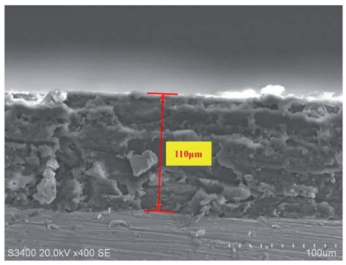

Fig. 4 SEM image of coating section.

It can be found from Fig. 5(a)–(e) that a relatively flat coating can be formed on the substrate surface when 0–3 wt% modified ZrO_2 is added to the epoxy coating. When the addition amount is more than 2 wt%, a large amount of ZrO_2 agglomerates on the coating surface, and the agglomeration of ZrO_2 is very serious when the content of ZrO_2 is 4 wt%. At the same time, more pores are generated on the coating surface, and the pore size becomes larger than other coatings, which destroy the dense structure of the coating. This is because when the added amount of ZrO_2 particles is too high, the nanoparticles will spontaneously attract each other and agglomerate into blocks. When the ZrO_2 content is 1–2 wt%, the agglomeration of ZrO_2 nanoparticles on the coating surface is not too severe. Among the five coatings, when the ZrO_2 content is 2 wt%, the modified ZrO_2 is most evenly dispersed on the coating surface, the number and size of pores on the coating surface are much lower than other coatings, the agglomeration of nanoparticles is less, and the surface shows the best compactness. This shows that there is good compatibility between the epoxy resin and modified ZrO_2 nanoparticles.

3.4 Corrosion resistance of coating

In order to obtain the optimum content of modified ZrO_2 filler in the epoxy coating, the corrosion resistance of the five

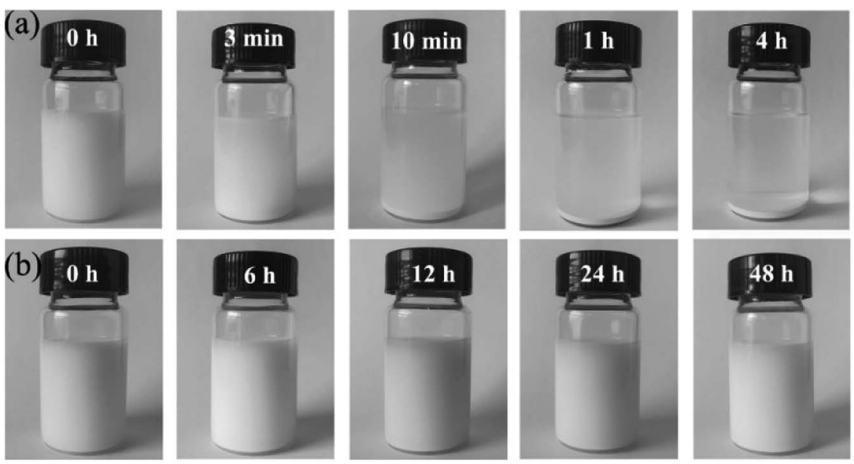

Fig. 3 Photographs of sedimentation process of (a) unmodified ZrO_2 and (b) APTES-modified ZrO_2 dispersed in anhydrous alcohol at different times.

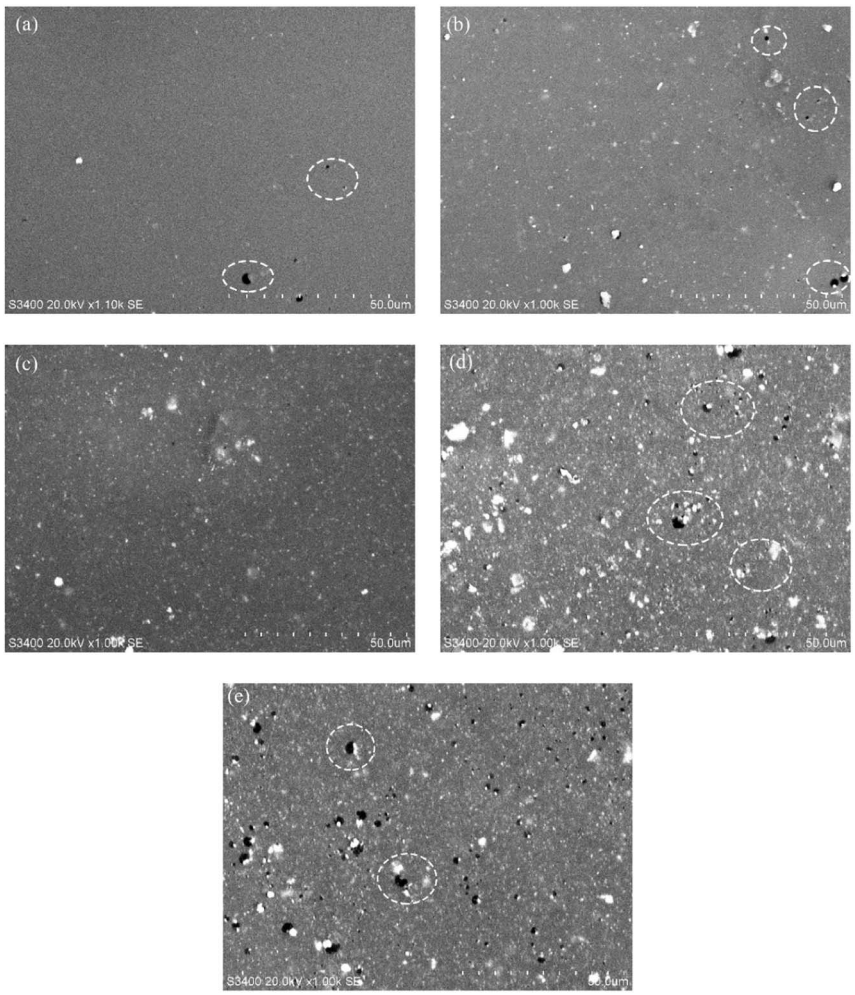

Fig. 5 The surface morphologies of epoxy coatings doped with different contents of modified ZrO_2 fillers are: (a) 0 wt%, (b) 1 wt%, (c) 2 wt%, (d) 3 wt%, (e) 4 wt%.

coatings and matrix in 3.5 wt% NaCl solution was studied *via* polarization curves and electrochemical impedance spectroscopy (EIS).

3.4.1 Polarization curve analysis. Fig. 6 shows the polarization curve of the Q235 steel plate and epoxy resin coating with 0–4 wt% modified ZrO_2 immersed in 3.5 wt% NaCl solution for 30 min. The corrosion potential (E_{corr}) and corrosion current density (I_{corr}) of the coating and substrate are fitted by the least square method. The main corrosion parameters after fitting are shown in Table 1, where E_{corr} represents corrosion potential and I_{corr} represents corrosion current. In general, higher E_{corr} and lower I_{corr} indicate better corrosion resistance of the coating.

The corrosion potential E_{corr} of the five coating samples decreased initially and then increased along with the gradual increase in the modified ZrO_2 content. The E_{corr} of the five coatings were higher than that of the Q235 steel plate, and the I_{corr} was lower than that of the Q235 steel plate, indicating that spraying the coating on the Q235 steel plate can protect the substrate. The I_{corr} value of the epoxy resin coating sample containing 2 wt% ZrO_2 is 6.2299×10^{-7} A cm^{-2}, which is 1

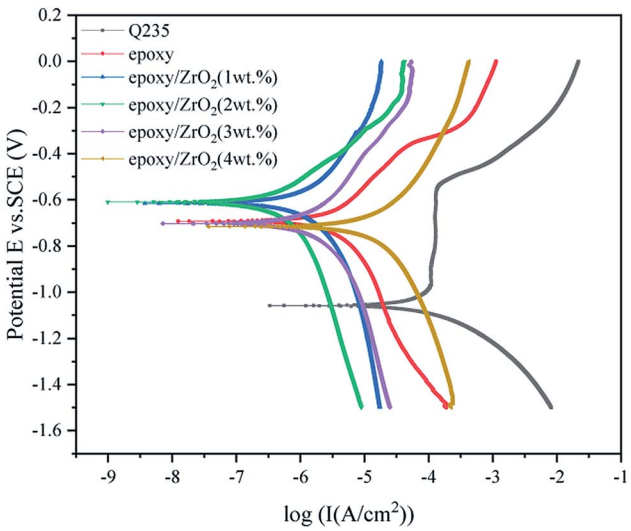

Fig. 6 Polarization curves of different samples in 3.5 wt% NaCl solution.

Table 1 Polarization parameters of different samples in 3.5 wt% NaCl solution

Sample	E_{corr} (V)	I_{corr} (A cm^{-2})
Q235	−1.0587	2.0695×10^{-4}
Epoxy	−0.69154	1.9105×10^{-5}
Epoxy/ZrO_2 (1 wt%)	−0.61533	6.0130×10^{-6}
Epoxy/ZrO_2 (2 wt%)	−0.60973	6.2299×10^{-7}
Epoxy/ZrO_2 (3 wt%)	−0.70182	1.9247×10^{-5}
Epoxy/ZrO_2 (4 wt%)	−0.71485	2.8199×10^{-5}

order of magnitude lower than the epoxy resin coating sample containing 1 wt% ZrO_2 and 2–3 orders of magnitude lower than the other samples. However, the I_{corr} containing 3–4 wt% is higher than that of pure epoxy coating.

3.4.2 Electrochemical impedance spectroscopy analysis. Six new groups of experimental samples were selected for the EIS test. Fig. 7 shows the EIS spectra of six samples after soaking for 30 min. In general, the radius of the capacitive resistance arc formed in the EIS curve can be used as the index of the corrosion rate. The larger the radius, the slower the corrosion rate and the stronger the corrosion resistance.[26,27] As seen from Fig. 7(a), when the addition amount of modified ZrO_2 is 2 wt%, the radius of the capacitive resistance arc in the Nyquist diagram is much larger than that of other coatings, indicating that the coating of this component has the best corrosion resistance. At the same time, in the Nyquist diagram, it can be found that the capacitive reactance arc radius increases first and then decreases with the increase in the amount of modified ZrO_2. From Fig. 7(b), the Bode diagram shows that the low frequency (0.01 Hz) impedance value of 2 wt% ZrO_2 epoxy coating is the largest, which is $1.0 \times 10^5\ \Omega\ cm^2$, more than other coatings. This may be because when the added amount of modified ZrO_2 is higher than 2 wt%, and due to the attraction between nanoparticles, they agglomerate with each other during the curing process, resulting in large pores on the coating surface. Corrosive substances such as water and Cl^- can penetrate through the pores and react directly with the metal, expanding the path from the corrosive medium to the matrix. At the same time, numerous nanoparticles will absorb water and swell in the solution, thus greatly increasing the internal stress between the particles and the coating. This will lead to the continuous penetration of the corrosive medium into the coating through these pores and the increase of the conductivity of the coating, resulting in the decline of coating performance. In general, the formation of corrosion reaction on the Q235 steel plate involves several steps and redox equations.[28]

$$Fe \rightarrow Fe^{2+} + 2e^-$$

$$Fe^{2+} \rightarrow Fe^{3+} + e^-$$

$$O_2(g) + 2H_2O + 4e^- \rightarrow 4OH^-$$

$$2Fe^{2+}(aq) + O_2(g) + 2H_2O \rightarrow 2FeOOH + 2H^+$$

It can be seen from the above equation that sufficient water and oxygen are required to dissolve steel to cause corrosion. If any of these processes is prevented, the corrosion will be inhibited and the coating can be effectively protected.[29] Although a small amount of modified ZrO_2 particles will agglomerate, they are evenly dispersed in the coating as a whole. In addition to this, the ZrO_2 particles after water absorption and swelling can tightly fill the gap of the coating, extending the path of corrosive medium into the coating, so as to inhibit the penetration of corrosive substances. The results show that the addition of excessive modified ZrO_2 nanoparticles to the epoxy coating will reduce the corrosion resistance of the coating.[30] The addition of 2 wt% modified ZrO_2 particles can improve the corrosion resistance of the epoxy coating.

Fig. 8 is an equivalent circuit for fitting the EIS results of modified ZrO_2 epoxy resin coatings with different contents. R_s, CPE_{coat}, R_{pore}, CPE_{dl} and R_{CT} in the figure represent solution resistance, coating constant phase element, coating gap resistance, double-layer constant phase resistance and charge transfer

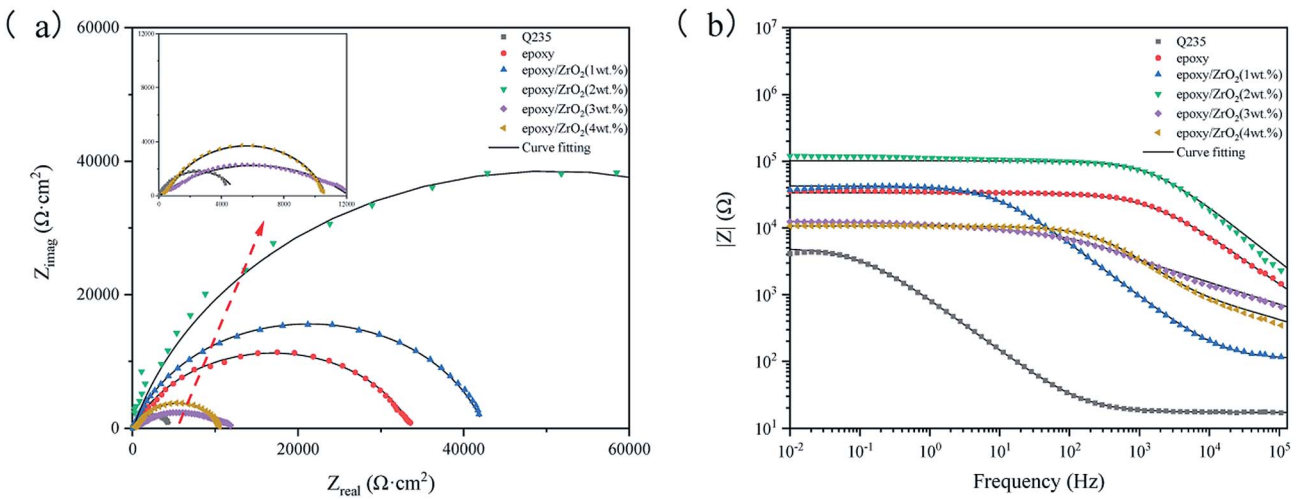

Fig. 7 EIS diagram of samples in 3.5 wt% NaCl solution (a) Nyquist diagram and (b) Bode diagram.

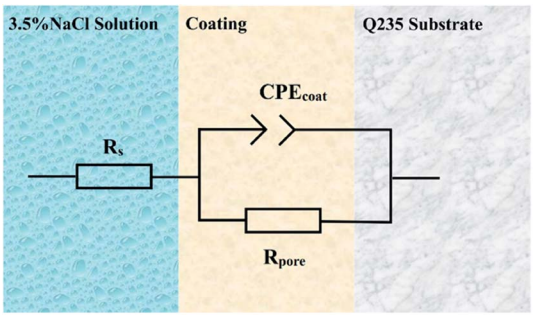

Fig. 8 Equivalent electrical circuit.

resistance, respectively. The constant phase element (CPE) represents the deviation from the ideal capacitance characteristics. Its function in the equivalent circuit is to reduce the system error and obtain more valuable fitting results. CPE is associated with dispersion index n ($0 \leq n \leq 1$). If $n = 1$, it represents an ideal capacitor, and if $n = 0$, it represents an ideal resistance.

Table 2 shows the fitting results of EIS after equivalent circuit fitting. The impedance value of ZrO_2 epoxy coating is 100 530 Ω cm^2, and the fitted data is consistent with the EIS curve. The electrochemical impedance spectra of the coating immersed in 3.5% NaCl solution for 30 min showed a time constant. At this time, the corrosive medium did not reach the Q235 matrix, and the addition amount was 3–4 wt%. The composite coating showed poor corrosion resistance after water absorption and swelling, which widened the corrosion path. Table 2 The parameters fitted by the equivalent circuit.

3.4.3. Corrosion mechanism of coating. Fig. 9 shows the anti-corrosion mechanism diagram of the coating. Fig. 9(a) is the corrosion mechanism of the pure epoxy resin coating. The defects of the epoxy resin can make the corrosion medium directly penetrate into the contact surface between the coating and the substrate, resulting in corrosion on the metal surface. Fig. 9(b) is the corrosion mechanism diagram when the content of nano zirconia particles added is large (3–4 wt%). Due to the addition of more nano zirconia particles in the resin coating, additional nano zirconia particles will be irregularly distributed in the coating. These nanoparticles will produce a large number of agglomeration of nanoparticles on the surface and inside of the coating, resulting in the widening of the inherent channel for corrosive ions and molecules to reach the gold surface,[31,32] and in defects in the composite coating. At the same time, the aggregates on the surface and inside of the coating will absorb water and swell during immersion, which increases the volume of the aggregates, creates a gap between the particles, and provides a new channel for the penetration of corrosive media. These will lead to the continuous penetration of corrosive media into the coating through the pores, increase the conductivity of the coating, and reduce the performance of the coating. Fig. 9(c) shows the corrosion resistance mechanism of the composite coating with a low content (1–2 wt%) of nano zirconia. As seen from Fig. 9(c), nano zirconia particles are evenly distributed in the coating, and the path of the corrosive medium penetrating into the bottom of the coating becomes longer,[33–35] which means that the time for the corrosive medium to reach the metal matrix will also become longer, which improves the corrosion resistance of the coating. The main reason is that the lower content of nano zirconia particles can disperse more evenly in the coating and the agglomeration phenomenon is significantly reduced. Moreover, due to the characteristics of nano zirconia being insoluble in water, when the agglomeration phenomenon is reduced, fewer particles can effectively fill the micropores and pores formed in the curing process of the composite coating. This improves the compactness of the coating, so as to hinder the infiltration path of corrosive media, make the diffusion rate of some corrosive media such as chloride ions, and also, delay the corrosion time of metal substrate.

Table 2 The parameters fitted by the equivalent circuit

		CPE$_{coat}$		
Sample	R_s, Ω cm^2	Y_0, Ω^{-1} cm^{-2} s^n	n	R_{pore}, Ω cm^2
Q235	17.08	2.6847×10^{-4}	0.78805	5025
Epoxy	88.33	3.1341×10^{-8}	0.74948	33 688
Epoxy/ZrO_2 (1 wt%)	107.0	9.1509×10^{-7}	0.80834	42 446
Epoxy/ZrO_2 (2 wt%)	97.4	3.478×10^{-9}	0.87076	100 530
Epoxy/ZrO_2 (3 wt%)	76.8	4.7327×10^{-6}	0.45024	12 155
Epoxy/ZrO_2 (4 wt%)	92.7	2.7722×10^{-7}	0.78914	10 289

3.4.4 Comparison between this work and other nanocomposite coatings. From Table 3, we can see that most epoxy resin coatings are accompanied by the escape of volatile organic compounds (VOCs) in the preparation process, but this

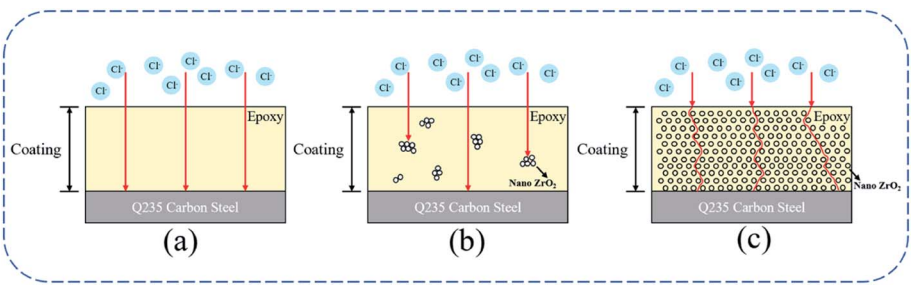

Fig. 9 Corrosion protection mechanism of coatings: (a) pure epoxy, (b) 3–4 wt% zirconia, (c) 1–2 wt% zirconia.

Table 3 Comparison between this work and other nanocomposite coatings

	Nanoparticles	Sample preparation method	VOC	Optimum addition
This work	ZrO_2	Electrostatic spraying	✗	2 wt%; 100 kΩ cm^2
Mariana do Nascimento Silva, *et al.*, 2020 (ref. 36)	RGO/graphite	Spraying	✓	0.5 wt%
Joseph Raj Xavier, 2019 (ref. 37)	MoO_3	Coated using a draw down bar	✓	2 wt%; 217 kΩ cm^2
G. Boomadevi Janaki, *et al.*, 2020 (ref. 38)	Al_2O_3	Coated using a draw down bar	✓	2 wt%; 208 kΩ cm^2
ChuanChun Li, *et al.*, 2020 (ref. 39)	Zn	Dip coating	✓	3 wt%
Weihang Li, *et al.*, 2020 (ref. 40)	TiO_2-GO	Brushing	✓	0.1 wt%; 1.5×10^{10} Ω cm^2
Mingshuai Guo, *et al.*, 2021 (ref. 41)	Al-PTFE	Brushing	✗	—
Diksha Dileep Thiruvoth, *et al.*, 2021 (ref. 42)	CeO_2	Doctor blades method	✓	1 wt%
Shuai Wang, *et al.*, 2020 (ref. 43)	Graphene	Dip coating	✗	0.5 wt%

phenomenon can be avoided by the electrostatic spraying technology.

4. Conclusion

In this study, nano ZrO_2 was modified by 3-aminopropyl triethoxysilane (APTES) and used as nano fillers to improve the corrosion resistance of epoxy coating. FTIR and static experimental results show that APTES has been successfully anchored on the surface of nano ZrO_2 particles through chemical bonds, and the modified ZrO_2 nanoparticles have good dispersion in ethanol solution. From the SEM image, it can be known that the thickness of the coating is about 110 μm. The surface morphology of the coating with 1–2 wt% modified ZrO_2 nanoparticles is dense. The electrochemical test results show that due to the barrier effect of nanoparticles, adding 1–2 wt% modified ZrO_2 nanoparticles to the epoxy coating can improve the protective performance of the epoxy coating. However, due to the increase in the amount of ZrO_2 nanoparticles, severe agglomeration can occur between the nanoparticles, which will reduce the corrosion resistance of the coating.

Conflicts of interest

The authors declared that they have no conflicts of interest to this work.

Acknowledgements

The authors would like to acknowledge the financial support from the National Natural Science Foundation of China (12062020) and the Natural Science Foundation of Inner Mongolia Autonomous Region of China (2019MS01016).

References

1 X. Ye, Z. Wang, L. Ma, *et al.*, Zinc oxide array/polyurethane nanocomposite coating: fabrication, characterization and corrosion resistance, *Surf. Coat. Technol.*, 2019, **358**, 497–504.
2 D. J. Mills, S. S. Jamali and K. Paprocka, Investigation into the effect of nano-silica on the protective properties of polyurethane coatings, *Surf. Coat. Technol.*, 2012, **209**, 137–142.
3 D. L. Song, S. Q. Liu, F. Li, Y. L. Wang, T. Zhang, Y. D. Yan, M. Zhang and J. Wang, Effects of Silane. modified Nano ZrO2 on the Corrosion Resistance of Epoxy Coating on the Surface of Mg-Li Alloy, *Chem. J. Chin. Univ.*, 2017, **38**(1), 77–84.
4 A. Olad, M. Barati and S. Behboudi, Preparation of PANI/epoxy/Zn nanocomposite using Zn nanoparticles and epoxy resin as additives and investigation of its corrosion protection behavior on iron[J], *Prog. Org. Coat.*, 2012, **74**(1), 221–227.
5 A. M. Atta, A. M. El-Saeed, G. M. El-Mahdy and H. A. Al-Lohedan, Application of magnetite nano-hybrid epoxy as protective marine coatings for steel, *RSC Adv.*, 2015, **5**(123), 101923–101931.
6 A. M. Atta, A. M. El-Saeed, H. I. Al-Shafey, H. A. Al-Lohedan, A. M. Tawfeek and M. Wahbey, Effect of Inorganic Nanomaterials Types Functionalized with Smart Nanogel on Anti-corrosion and Mechanical Performances of Epoxy Coatings, *Int. J. Electrochem. Sci.*, 2017, **12**(2), 1167–1182.
7 D. C. Xue and W. J. Van Ooij, Corrosion performance improvement of hot-dipped galvanized (HDG) steels by electro-deposition of epoxy-resin-ester modified bis-[triethoxy-silyl] ethane (BTSE) coatings, *Prog. Org. Coat.*, 2013, **76**(7–8), 1095–1102.
8 H. E. Mohammadloo, A. A. Sarabi, H. R. Asemani and P. Ahmadi, A comparative study of eco-friendly hybrid thin films: With and without organic coating application, *Prog. Org. Coat.*, 2018, **125**, 432–442.
9 A. Kumar, R. Anant, K. Kumar, S. S. Chauhan, S. Kumar and R. Kumar, Anticorrosive and electromagnetic shielding response of a graphene/TiO2-epoxy nanocomposite with enhanced mechanical properties, *RSC Adv.*, 2016, **6**(114), 113405–113414.
10 Z. B. Wang, Z. Y. Wang, H. X. Hu, C. B. Liu and Y. G. Zheng, Corrosion Protection Performance of Nano-SiO2/Epoxy Composite Coatings in Acidic Desulfurized Flue Gas Condensates, *J. Mater. Eng. Perform.*, 2016, **25**(9), 3880–3889.
11 Y. Ma, H. H. Di, Z. X. Yu, L. Liang, L. Lv, Y. Pan, Y. Y. Zhang and D. Yin, Fabrication of silica-decorated graphene oxide nanohybrids and the properties of composite epoxy coatings research, *Appl. Surf. Sci.*, 2016, **360**, 936–945.
12 S. Wang, R. Ding, X. D. Zhao, Q. Fu, H. Sun, S. Y. Chen, Z. Y. An, Y. Li and X. L. Qu, Effect of Graphene Addition

on Anticorrosion Performance of Two Kinds of Epoxy Coatings, *Int. J. Electrochem. Sci.*, 2020, **15**(7), 7082–7092.

13 W. Sun, T. T. Wu, L. D. Wang, Z. Q. Yang, T. Z. Zhu, C. Dong and G. C. Liu, The role of graphene loading on the corrosion-promotion activity of graphene/epoxy nanocomposite coatings, *Composites, Part B*, 2019, **173**, 106916.

14 M. Kathalewar, A. Sabnis and G. Waghoo, Effect of incorporation of surface treated zinc oxide on non-isocyanate polyurethane based nano-composite coatings, *Prog. Org. Coat.*, 2013, **76**(9), 1215–1229.

15 W. H. Xu, Z. Y. Wang, E. H. Han, S. Wang and Q. Liu, Corrosion Performance of Nano-ZrO2 Modified Coatings in Hot Mixed Acid Solutions, *Materials*, 2018, **11**(6), 934.

16 E. Mahmoudi, S. H. Mohitfar and S. Mahdavi, Characteristics and corrosion behavior of as-deposited and heat-treated Co–Cr/ZrO2 coatings electrodeposited from Cr(III) baths, *Mater. Chem. Phys.*, 2021, **272**, 125030.

17 J. Chang, Z. Wang, E. H. Han, *et al.*Corrosion resistance of tannic acid, d-limonene and nano-ZrO2 modified epoxy coatings in acid corrosion environments, *J. Mater. Sci. Technol.*, 2020, **65**, 137–150.

18 M. Peron, S. Cogo, M. Bjelland, *et al.*On the evaluation of ALD TiO2, ZrO2 and HfO2 coatings on corrosion and cytotoxicity performances, *J. Magnesium Alloys*, 2021, **9**, 1806–1819.

19 U. Eduok, J. Szpunar and E. Ebenso, Synthesis and characterization of anticorrosion zirconia/acrylic nanocomposite resin coatings for steel, *Prog. Org. Coat.*, 2019, **137**(5), 105337.

20 X. Zhao, S. Liu, X. T. Wang and B. R. Hou, Surface modification of ZrO2 nanoparticles with styrene coupling agent and its effect on the corrosion behaviour of epoxy coating, *Chin. J. Oceanol. Limnol.*, 2014, **32**(5), 1163–1171.

21 A. M. Atta, M. A. Ahmed, A. M. El-Saeed, O. M. Abo-Elenien and M. A. El-Sockary, Hybrid ZrO2/Cr2O3 Epoxy Nanocomposites as Organic Coatings for Steel, *Coatings*, 2020, **10**(10), 997.

22 J. G. Checmanowski and B. Szczygiel, Effect of a ZrO2 coating deposited by the sol-gel method on the resistance of FeCrAl alloy in high-temperature oxidation conditions, *Mater. Chem. Phys.*, 2013, **139**(2–3), 944–952.

23 X. D. Lv, X. T. Li, N. Li, H. C. Zhang, Y. Z. Zheng, J. J. Wu and X. Tao, ZrO2 nanoparticle encapsulation of graphene microsheets for enhancing anticorrosion performance of epoxy coatings, *Surf. Coat. Technol.*, 2019, **358**, 443–451.

24 J. L. Li, C. Peng, Z. W. Li, Z. J. Wu and S. C. Li, The improvement in cryogenic mechanical properties of nano-ZrO2/epoxy composites *via* surface modification of nano-ZrO2, *RSC Adv.*, 2016, **6**(66), 61393–61401.

25 M. Behzadnasab, S. M. Mirabedini, K. Kabiri and S. Jamali, Corrosion performance of epoxy coatings containing silane treated ZrO2 nanoparticles on mild steel in 3.5% NaCl solution, *Corros. Sci.*, 2011, **53**(1), 89–98.

26 K. C. Chang, M. C. Lai, C. W. Peng, Y. T. Chen, J. M. Yeh, C. L. Lin and J. C. Yang, Comparative studies on the corrosion protection effect of DBSA-doped polyaniline prepared from *in situ* emulsion polymerization in the presence of hydrophilic Na+-MMT and organophilic organo-MMT clay platelets, *Electrochim. Acta*, 2006, **51**(26), 5645–5653.

27 E. Hur, G. Bereket and Y. Sahin, Anti-corrosive properties of polyaniline, poly(2-toluidine), and poly(aniline-co-2-toluidine) coatings on stainless steel, *Curr. Appl. Phys.*, 2007, **7**(6), 597–604.

28 S. Radhakrishnan, C. R. Siju, D. Mahanta, S. Patil and G. Madras, Conducting polyaniline-nano-TiO2 composites for smart corrosion resistant coatings, *Electrochim. Acta*, 2009, **54**(4), 1249–1254.

29 C. B. Hu, Y. S. Zheng, Y. Q. Qing, F. L. Wang, C. Y. Mo and Q. Mo, Preparation of Poly(o-toluidine)/Nano ZrO2/Epoxy Composite Coating and Its Application for Corrosion Protection of Steel, *J. Wuhan Univ. Technol.*, 2016, **31**(4), 937–944.

30 Y. J. Jing, P. Q. Wang, Q. B. Yang, Q. R. Wang and Y. Bai, MoS2 decorated with ZrO2 nanoparticles through mussel-inspired chemistry of dopamine for reinforcing anticorrosion of epoxy coatings, *Colloids Surf., A*, 2021, **608**, 125625.

31 S. Ammar, *et al.*, Studies on SiO2-hybrid polymeric nanocomposite coatings with superior corrosion protection and hydrophobicity, *Surf. Coat. Technol.*, 2017, **324**, 536–545.

32 M. Conradi, A. Kocijan, D. Kek-Merl, *et al.*, Mechanical and anticorrosion properties of nanosilica-filled epoxy-resin composite coatings, *Appl. Surf. Sci.*, 2014, **292**, 432–437.

33 B. Ramezanzadeh, S. Niroumandrad, A. Ahmadi, *et al.*, Enhancement of barrier and corrosion protection performance of an epoxy coating through wet transfer of amino functionalized graphene oxide, *Corros. Sci.*, 2016, **103**, 283–304.

34 U. Eduok, O. Faye, A. Tiamiyu, *et al.*, Fabricating protective epoxy-silica/CeO2 films for steel: Correlating physical barrier properties with material content[J], *Mater. Des.*, 2017, **124**, 58–68.

35 U. Eduok and J. Szpunar, Ultrasound-assisted synthesis of zinc molybdate nanocrystals and molybdate-doped epoxy/PDMS nanocomposite coatings for Mg alloy protection[J], *Ultrason. Sonochem.*, 2018, **44**, 288–298.

36 M. do Nascimento Silva, *et al.*, Corrosion behaviour of an epoxy paint reinforced with carbon nanoparticles, *Corros. Eng., Sci. Technol.*, 2020, **55**(8), 1767322.

37 J. R. Xavier, Investigation on the anticorrosion, adhesion and mechanical performance of epoxy nanocomposite coatings containing epoxy-silane treated nano-MoO3 on mild steel, *J. Adhes. Sci. Technol.*, 2019, 1–20.

38 G. B. Janaki and J. R. Xavier, Effect of indole functionalized nano-alumina on the corrosion protection performance of epoxy coatings in marine environment, *J. Macromol. Sci., Part A: Pure Appl.Chem.*, 2020, **57**(10), 691–702.

39 C. C. Li, T. Y. Lai and T. H. Fang, Corrosion Resistant Coatings Based on Zinc Nanoparticles, Epoxy and Silicone Resins, *J. Nanosci. Nanotechnol.*, 2020, **20**(10), 18709.

40 W. Li, B. Song, S. Zhang, *et al.*, Using 3-Isocyanatopropyltrimethoxysilane to Decorate Graphene Oxide with Nano-Titanium Dioxide for Enhancing the Anti-

Corrosion Properties of Epoxy Coating, *Polymers*, 2020, **12**(4), 837.

41 M. Guo, Electrochemical Corrosion Behaviour of Nano Aluminium - Polytetrafluoroethylene Pigment Modified Water borne Epoxy Coating on Carbon Steel, *Int. J. Electrochem. Sci.*, 2021, 150871.

42 D. Dileep Thiruvoth and M. Ananthkumar, Evaluation of cerium oxide nanoparticle coating as corrosion inhibitor for mild steel, *Mater. Today*, 2021, **49**(5), 2007–2012.

43 S. Wang, Effect of Graphene Addition on Anticorrosion Performance of Two Kinds of Epoxy Coatings, *Int. J. Electrochem. Sci.*, 2020, 7082–7092.